JCI insight

CX3CR1 identifies PD-1 therapy–responsive CD8$^+$ T cells that withstand chemotherapy during cancer chemoimmunotherapy

Yiyi Yan, … , Roxana S. Dronca, Haidong Dong

JCI Insight. 2018;3(8):e97828. https://doi.org/10.1172/jci.insight.97828.

Research Article | Immunology | Oncology

Although immune checkpoint inhibitors have resulted in durable clinical benefits in a subset of patients with advanced cancer, some patients who did not respond to initial anti–PD-1 therapy have been found to benefit from the addition of salvage chemotherapy. However, the mechanism responsible for the successful chemoimmunotherapy is not completely understood. Here we show that a subset of circulating CD8$^+$ T cells expressing the chemokine receptor CX3CR1 are able to withstand the toxicity of chemotherapy and are increased in patients with metastatic melanoma who responded to chemoimmunotherapy (paclitaxel and carboplatin plus PD-1 blockade). These CX3CR1$^+$CD8$^+$ T cells have effector memory phenotypes and the ability to efflux chemotherapy drugs via the ABCB1 transporter. In line with clinical observation, our preclinical models identified an optimal sequencing of chemoimmunotherapy that resulted in an increase of CX3CR1$^+$CD8$^+$ T cells. Taken together, we found a subset of PD-1 therapy–responsive CD8$^+$ T cells that were capable of withstanding chemotherapy and executing tumor rejection with their unique abilities of drug efflux (ABCB1), cytolytic activity (granzyme B and perforin), and migration to and retention (CX3CR1 and CD11a) at tumor sites. Future strategies to monitor and increase the frequency of CX3CR1$^+$CD8$^+$ T cells may help to design effective chemoimmunotherapy to overcome cancer resistance to immune checkpoint blockade therapy.

JCI insight

RESEARCH ARTICLE

CX3CR1 identifies PD-1 therapy–responsive CD8⁺ T cells that withstand chemotherapy during cancer chemoimmunotherapy

Yiyi Yan,[1] Siyu Cao,[2] Xin Liu,[2] Susan M. Harrington,[2] Wendy E. Bindeman,[2] Alex A. Adjei,[1,3] Jin Sung Jang,[4] Jin Jen,[4] Ying Li,[5] Pritha Chanana,[5] Aaron S. Mansfield,[1] Sean S. Park,[6] Svetomir N. Markovic,[1] Roxana S. Dronca,[1] and Haidong Dong[2,7]

[1]Division of Medical Oncology, [2]Department of Urology, [3]Mayo Clinic Cancer Center Early Therapeutic Program, [4]Mayo Clinic Center of Individualized Medicine, [5]Department of Biomedical Statistics and Informatics, [6]Department of Radiation Oncology, and [7]Department of Immunology, Mayo Clinic, Rochester, Minnesota, USA.

Although immune checkpoint inhibitors have resulted in durable clinical benefits in a subset of patients with advanced cancer, some patients who did not respond to initial anti–PD-1 therapy have been found to benefit from the addition of salvage chemotherapy. However, the mechanism responsible for the successful chemoimmunotherapy is not completely understood. Here we show that a subset of circulating CD8⁺ T cells expressing the chemokine receptor CX3CR1 are able to withstand the toxicity of chemotherapy and are increased in patients with metastatic melanoma who responded to chemoimmunotherapy (paclitaxel and carboplatin plus PD-1 blockade). These CX3CR1⁺CD8⁺ T cells have effector memory phenotypes and the ability to efflux chemotherapy drugs via the ABCB1 transporter. In line with clinical observation, our preclinical models identified an optimal sequencing of chemoimmunotherapy that resulted in an increase of CX3CR1⁺CD8⁺ T cells. Taken together, we found a subset of PD-1 therapy–responsive CD8⁺ T cells that were capable of withstanding chemotherapy and executing tumor rejection with their unique abilities of drug efflux (ABCB1), cytolytic activity (granzyme B and perforin), and migration to and retention (CX3CR1 and CD11a) at tumor sites. Future strategies to monitor and increase the frequency of CX3CR1⁺CD8⁺ T cells may help to design effective chemoimmunotherapy to overcome cancer resistance to immune checkpoint blockade therapy.

Introduction

Considering that most patients will not show major durable responses to immunotherapy, management after PD-1 blockade failure remains a pressing challenge in the clinic (1). A substantial effort is currently underway to fully elucidate the mechanisms by which these immune checkpoint inhibitors exert their efficacy and to further explore the potential synergy of combination therapies in order to overcome low clinical efficacy or acquired resistance to anti–PD-1/PD-L1 (anti–PD-1/L1) monotherapy. Combination strategies (e.g., with chemotherapy) have been tested in clinical practice after disease progression on anti–PD-1 therapy. For patients with non–small cell lung cancer (NSCLC), combinations of chemotherapy with PD-1 and PD-L1 inhibitors have shown promising antitumor activities and a manageable, nonoverlapping toxicity profile (2). Recently, it has been shown that the addition of pembrolizumab to carboplatin and pemetrexed improves efficacy and has a favorable risk profile in patients with chemotherapy-naive metastatic NSCLC (3). In metastatic melanoma patients who received anti–PD-1 therapy (pembrolizumab), we found that approximately 26% demonstrated an objective response to subsequent chemotherapy (including carboplatin and paclitaxel [CP]) compared with a lower response rate in chemotherapy-only historic controls (4, 5). Similar findings have been reported in NSCLC (6, 7). However, the mechanism responsible for these successful clinical outcomes of chemoimmunotherapy (CIT) is not completely understood.

The antitumor effects of chemotherapy are achieved mainly through direct killing of cancer cells via various mechanisms. The immune-regulatory effects of chemotherapy also contribute to its antitumor activities.

Authorship note: YY and SC are co–first authors. RSD and HD are co–senior authors.

Conflict of interest: The authors have declared that no conflict of interest exists.

Submitted: October 2, 2017
Accepted: March 20, 2018
Published: April 19, 2018

Reference information:
JCI Insight. 2018;3(8):e97828. https://doi.org/10.1172/jci.insight.97828.

For example, tumor antigens released upon chemotherapy-induced immunogenic cell death can enhance cytotoxic T cell responses, thereby improving immunotherapy outcomes (8). On the other hand, chemotherapy-induced lymphopenia augments antitumor immunity by potentiating antigen-specific T cell responses, particularly during the recovery phase from lymphopenia (9–11). The antitumor effects of conventional cancer chemotherapy may also result from its ability to disrupt immune suppressive pathways, such as depletion of Tregs (12, 13) and other immunosuppressive cell populations (e.g., myeloid-derived suppressor cells), elimination of endogenous cytokine sinks for homeostatic cytokines, and enhanced proliferation of effector or memory T cells (10, 14). Although chemotherapeutic agents promote antitumor immunity through induction of immunogenic cell death in tumors and depletion of other immunosuppressor cells (15, 16), the impact of chemotherapy drugs on the function of PD-1 therapy–responsive T cells is largely unknown. Since these T cells are the main mediators of the antitumor activity of immune checkpoint inhibitors (17–19), it is critical to understand how tumor-reactive T cells respond to CIT in order to develop a rational CIT protocol to overcome tumor resistance to anti–PD-1 monotherapy.

We have been developing markers to identify human tumor–reactive T cells (19) and to monitor T cell responses to anti–PD-1 therapy in melanoma patients (20). In this report, we found that $CX3CR1^+CD8^+$ T cells represent a subset of PD-1 therapy–responsive $CD8^+$ T cells that exhibits an effector memory phenotype and withstands chemotherapy in cancer patients who are responsive to CIT. Thus, our results provide new insights to T cell responses to CIT in cancer patients.

Results

Patients who have failed PD-1 blockade benefit from CIT. A large fraction of cancer patients (60%–70%) who receive PD-1 blockade alone are resistant to PD-1 therapy or experience subsequent disease progression (21–23); however, some of them benefit from late-line or salvage treatment with conventional chemotherapy. Ever since the safety and efficacy profile of CIT have been demonstrated in NSCLC patients (2, 3), we have treated a number of patients who have evidence of disease progression on initial PD-1 blockade monotherapy with subsequent chemotherapy, in addition to continuing anti–PD-1 antibody beyond progression (4). To minimize toxicities, a short course of chemotherapy (2–6 cycles) was combined with anti–PD-1 therapy, which was maintained thereafter. Among 22 patients who did not respond to anti–PD-1 monotherapy and received subsequent addition of CP, a complete response rate of 23% was observed at a median follow-up of 3.9 years, according to the Response Evaluation Criteria in Solid Tumors (RECIST) criteria (Y. Yan, R.S. Dronca, and H. Dong, unpublished clinical observations).

CX3CR1 expression increased in PD-1 therapy–responsive $CD8^+$ T cells in the peripheral blood of metastatic melanoma patients receiving CIT. The clinical success of subsequent CIT in patients who did not respond to initial anti–PD-1 monotherapy prompted us to seek predictive biomarkers to select potential responders in order to increase the efficacy of CIT. First, we examined which subsets of $CD8^+$ T cells in the peripheral blood of cancer patients would be responsive to anti–PD-1 monotherapy. Secondly, we examined whether this responsive T cell population would be preserved during chemotherapy and still retain responsiveness to PD-1 blockade. To that end, we performed RNA sequencing (RNA-seq) analysis of $CD11a^{hi}CD8^+$ T cells isolated and sorted from patients' peripheral blood, a population containing enriched tumor-reactive T cells (19), and compared gene transcription between responders and nonresponders prior to (baseline) and after (upon first disease response assessment, i.e., 3 months later) PD-1 therapy. At baseline, we found CX3CR1 as one of the top genes that showed higher expression (ratio >1.5) in responders compared with nonresponders (Figure 1A). Of note, there was overrepresentation of TCRβ V29-1 among $CD11a^{hi}PD\text{-}1^+CD8^+$ T cells in responders prior to PD-1 therapy, suggesting that there might be a monoclonal expansion of tumor-reactive T cells that would eventually be responsive to anti–PD-1 therapy.

We then compared the gene expression in $CD11a^{hi}CD8^+$ T cells isolated and sorted from the peripheral blood of responders and nonresponders 3 months after anti–PD-1 treatment. As shown in Figure 1B, the responders harbored more effector memory $CD8^+$ T cells than nonresponders based on their higher (>2-fold change) expression of CX3CR1, CD122 (IL-2Rβ chain), KLRG1 (effector differentiation marker), perforin, and granzyme B (effector molecules). However, IFN-γ expression was unexpectedly increased in $CD8^+$ T cells of nonresponders rather than in responders. Despite its role in antitumor activity, IFN-γ plays a role in inducing apoptosis of effector cells and limiting memory cell generation (24–26). In line with these observations, our results warrant further scrutiny of the role of IFN-γ expressed by tumor-reactive T cells in response to anti–PD-1 therapy. Interestingly, a recent report found increased levels of IFN-γ in the

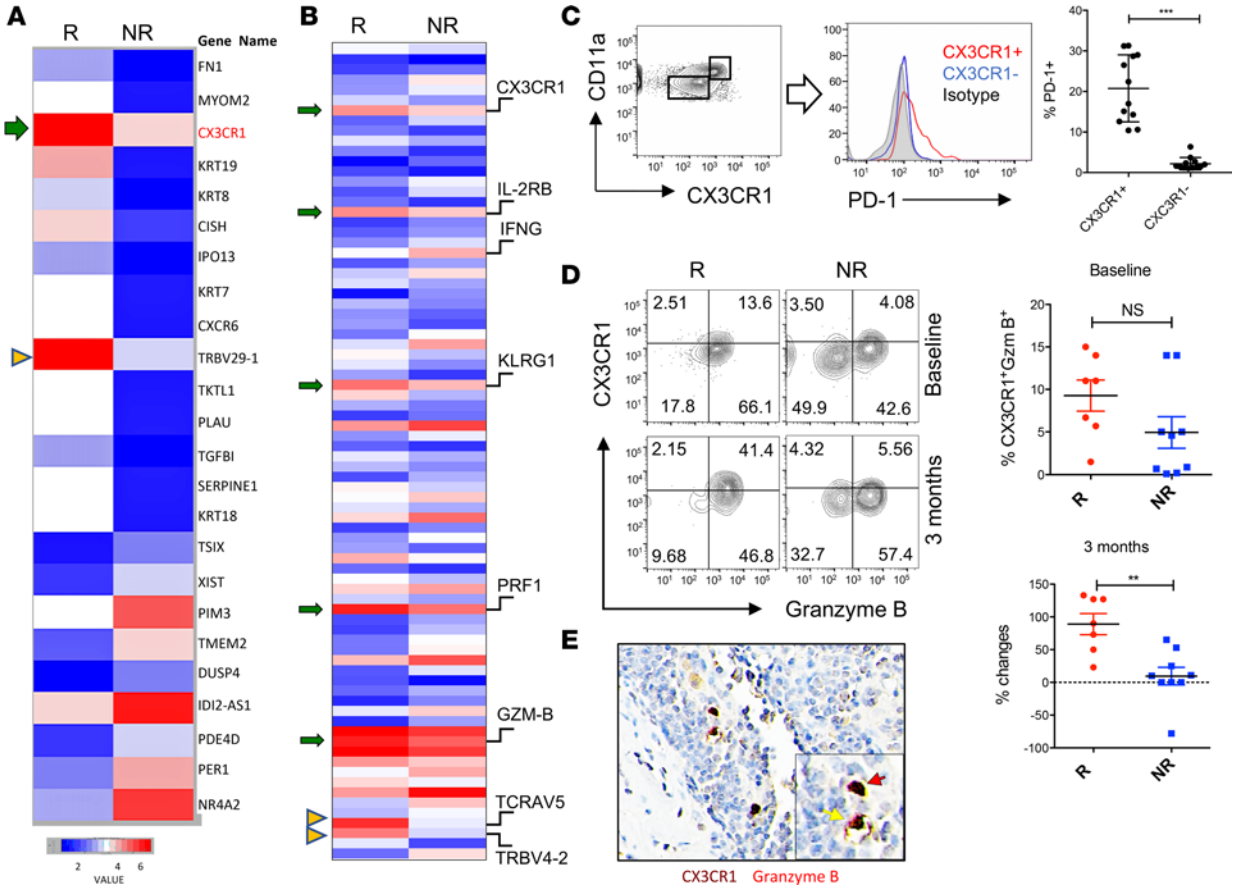

Figure 1. CX3CR1⁺Granzyme B⁺CD8⁺ T cells in responders to PD-1 therapy. RNA was isolated from CD11a^{hi}CD8⁺ T cells in the peripheral blood of melanoma patients prior to (**A**) or after (**B**) anti–PD-1 therapy. (**A**) RNA-seq data show an increased transcription of CX3CR1 (arrow) and TCRVβ29-1 (arrow head) in the responders (R, *n* = 3) compared with the nonresponders (NR, *n* = 3) at baseline prior to anti–PD-1 therapy. Data represent the average levels of transcription of 3 patients (with at least 1.5-fold changes). (**B**) RNA-seq data show increased transcriptions of CX3CR1, CD122 (IL2RB), KLRG1, perforin (PRF1), granzyme B (GZMB) (arrows), and TCRVα5/TCRVβ4-2 (arrow heads) on week 12 after PD-1 therapy. Data represent the average levels of transcription of 3 or 2 patients (R, *n* = 3; NR, *n* = 2) with at least 2-fold changes. (**C**) PD-1 expression by CX3CR1⁺CD11a^{hi} or CX3CR1⁻CD11a^{lo} CD8⁺ T cells isolated from the peripheral blood of patients with metastatic melanoma prior to PD-1 therapy (*n* = 12, ***$P < 0.01$, paired 2-tailed *t* test). (**D**) The frequency of CX3CR1⁺Granzyme B⁺ cells among CD11a^{hi}CD8⁺ T cells significantly increased in responders after anti–PD-1 therapy in melanoma patients (*n* = 7, **$P < 0.05$, Mann-Whitney *U* test) but not at baseline prior to PD-1 therapy. (**E**) Tissue staining of CX3CR1⁺Granzyme B⁺ (double-positive staining, DP) in human melanoma tissues. Original magnification ×400. One DP cell was inside the tumor bed (red arrow) and another adhered to a blood vessel, probably in a process of extravasation (yellow arrow).

plasma of nonresponders to PD-1 therapy (27). Although we performed RNA-seq analysis on a different cohort of patients (Figure 1B), the increase of CX3CR1 expression was consistent with what we found at baseline (Figure 1A). Interestingly, we observed overrepresentation of TCRVα5 and TCRVβ4-2 among CD11a^{hi}CD8⁺ T cells in responders after PD-1 therapy, suggesting that anti–PD-1 therapy promoted an oligoclonal expansion of tumor-reactive T cells.

To confirm whether CX3CR1⁺CD8⁺ T cells are the cellular targets of anti–PD-1 therapy, we measured and compared the expression of PD-1 among CX3CR1⁺ or CX3CR1⁻ CD8⁺ T cells. As shown in Figure 1C, PD-1 was mainly expressed by CX3CR1⁺CD8⁺ T cells rather than CX3CR1⁻CD8⁺ T cells. Since CX3CR1 and granzyme B have been used to identify human effector memory CD8⁺ T cells during viral infections (28), we tested whether CX3CR1⁺Granzyme B⁺ cells can be used to identify a subset of CD8⁺ T cells in the peripheral blood of cancer patients in response to anti–PD-1 immunotherapy. We found the frequency of CX3CR1⁺Granzyme B⁺ cells increased in responders compared with nonresponders after anti–PD-1 treatment but not at the baseline (prior to PD-1 therapy) (Figure 1D). In resected metastatic melanoma tissue biopsies obtained prior to PD-1 therapy, we identified CX3CR1⁺Granzyme B⁺ (double-positive; DP) cells that were infiltrating tumor tissues (Figure 1E). Interestingly, CX3CR1⁺Granzyme B⁺ cells appeared in a blood vessel within the tumor tissue, suggest-

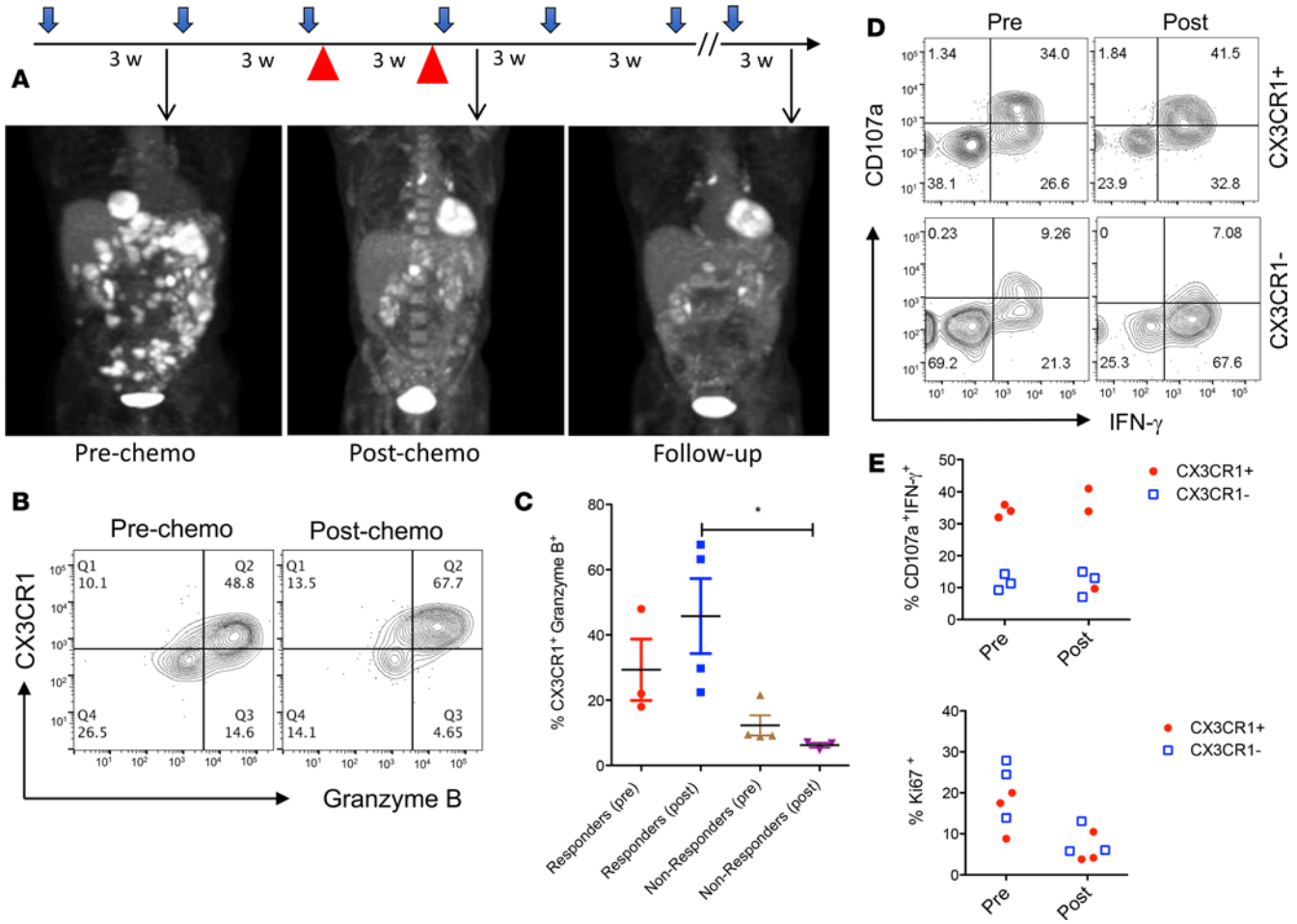

Figure 2. Patient responses to chemoimmunotherapy with an increase of CX3CR1⁺Granzyme B⁺CD8⁺ T cells. (**A**) Treatment schedule and clinical responses of a patient with metastatic melanoma who received pembrolizumab single-agent and chemotherapy paclitaxel and carboplatin (red arrow head) that were initiated at 175 mg/m², and an AUC (area under curve) of 5 every 3 weeks for 2 cycles in combination with pembrolizumab. PET/CT scan results were collected at each time point (arrows) to demonstrate the disease status. Patient received a total of 12 cycles of pembrolizumab at the end of follow up, shown here. (**B**) Following the same schedule of treatment as in **A**, blood samples were collected for flow analysis of CX3CR1⁺Granzyme B⁺ among CD11a^{hi}CD8⁺ T cells. (**C**) The frequency of CX3CR1⁺Granzyme B⁺ among CD11a^{hi}CD8⁺ T cells in responders (n = 3 pre, 4 post) and nonresponders (n = 4) before and after chemotherapy as treated in **A**. *P < 0.05 compared between responders and nonresponders to CIT (1-way ANOVA, P = 0.024). (**D**) Representative flow cytometry data showing the CTL function of CX3CR1⁺ or CX3CR1⁻ CD8⁺ T cells from one of the chemoimmunotherapy responders (n = 3) after a brief ex vivo stimulation of T cells with PMA and ionomycin. (**D** and **E**) CTL function (CD107a expression and IFN-γ production) and proliferation (Ki67 expression) of CX3CR1⁺ or CX3CR1⁻ CD8⁺ T cells in responders (n = 3) prior to and after PD-1 therapy.

ing a potential extravasation of CX3CR1⁺Granzyme B⁺ cells into tumor sites from systemic circulation. Taken together, our results demonstrate that CX3CR1 identifies a subset of CD8⁺ T cells that are responsive to anti–PD-1 therapy and have the potential to migrate into tumor tissues.

CX3CR1⁺Granzyme B⁺CD8⁺ T cells increased in the peripheral blood of responders after CIT. Next, we examined the frequency of CX3CR1⁺Granzyme B⁺CD8⁺ T cells before and after chemotherapy administration as part of the combination with anti–PD-1 blockade in patients with metastatic melanoma. As shown in Figure 2A, 1 patient had rapid progression of metastatic melanoma in the peritoneum and liver while on treatment with anti–PD-1 antibody (pembrolizumab) alone, so CP (3 weeks/cycle) were initiated and continued with pembrolizumab. Three weeks after the combination therapy, this patient demonstrated dramatically reduced tumor lesions. Importantly, chemotherapy was stopped after 2 cycles, and this patient experienced ongoing clinical benefits with maintenance of single-agent anti–PD-1 immunotherapy. To test whether CX3CR1⁺Granzyme B⁺CD8⁺ cells were preserved during chemotherapy and still responsive to anti–PD-1 therapy, we measured the frequency of circulating CX3CR1⁺Granzyme B⁺CD8⁺ T cells before and after the chemotherapy in this patient (time points shown in Figure 2A). One week after the addition of chemotherapy, the frequency of CX3CR1⁺Granzyme B⁺ cells increased among CD11a^{hi}CD8⁺ T cells in this patient,

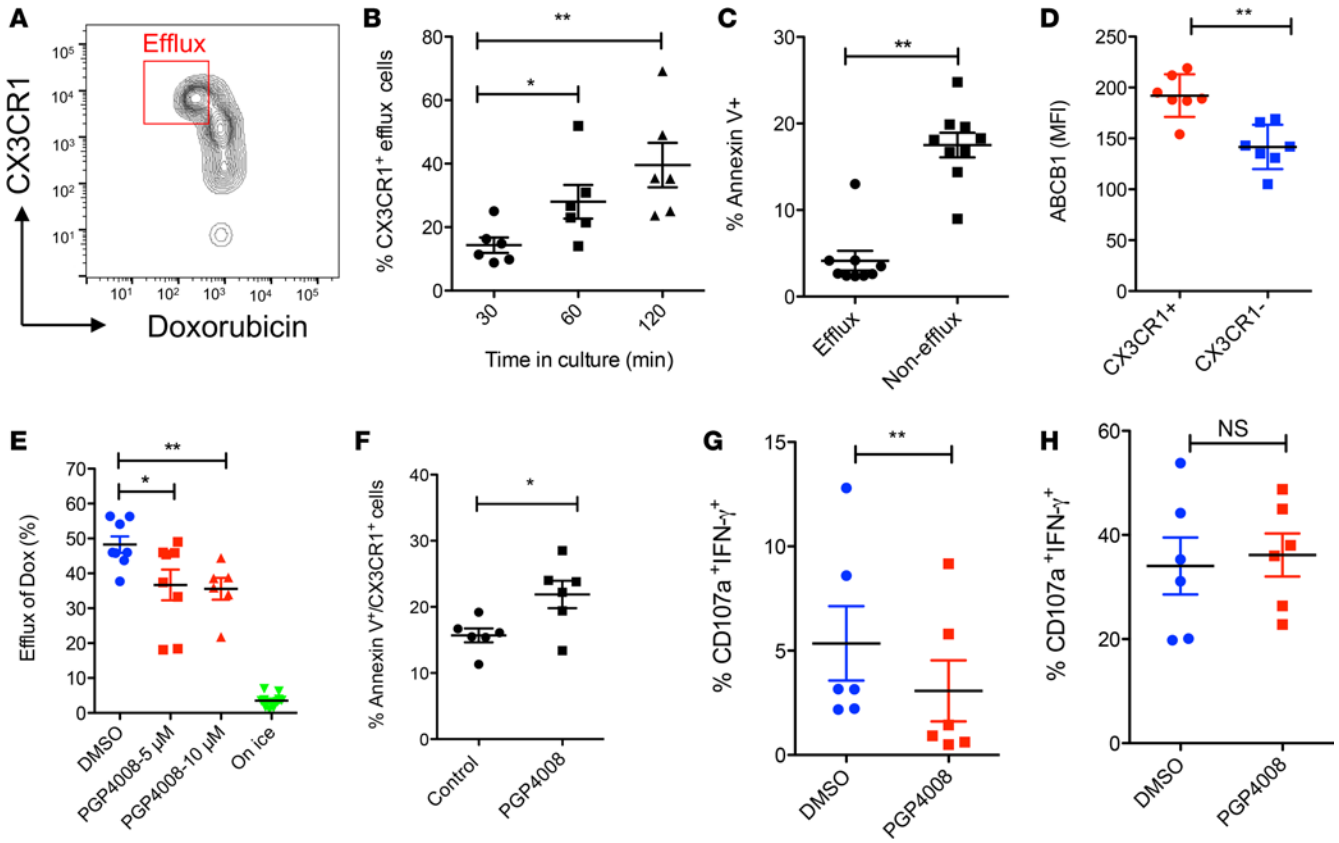

Figure 3. Efflux of chemotherapy drug by human CX3CR1$^+$CD8$^+$ T cells. Purified human primary CD8$^+$ T cells were loaded with Doxorubicin (1 μg/ml) for 30 minutes and then washed before further incubation for 60 minutes (**A**) or at indicated times (**B**). Gated areas in **A** are efflux cells (Dox^{lo}CX3CR1^{hi}). The data was analyzed by 1-way ANOVA (*$P < 0.05$, **$P < 0.01$, $n = 6$). (**C**) CD8$^+$ T cells were incubated with Doxorubicin (0.5 μg /ml) for 40 hours and then stained with annexin V to identify apoptotic cells. (**D**) Expression of ABCB1 by CX3CR1$^+$ or CX3CR1$^-$ CD8$^+$ T cells. (**E**) ABCB1 inhibitor (PGP4008) reduced the drug efflux ability of CX3CR1$^+$CD8$^+$ T cells. Cells incubated on ice after loading with drug were used as a negative control for drug efflux. Data was analyzed by 1-way ANOVA (*$P < 0.05$, **$P < 0.01$, $n = 7$). (**F**) ABCB1 inhibitor (PGP4008) increased the apoptosis of CX3CR1$^+$CD8$^+$ T cells as cultured in **C**. The impact of ABCB1 inhibitor on the function of human CX3CR1$^+$CD8$^+$ T cells incubated with (**G**) or without (**H**) chemotherapy drug (carboplatin and paclitaxel). CD8$^+$ T cells were activated with anti-CD3/CD28 beads for 24 hours in the presence of DMSO (control) or PGP4008 (10 μM). The CTL function was measured for CD107a expression and IFN-γ production at the end of culture. The data of **C**–**D** and **F**–**H** were analyzed by Mann-Whitney *U* test, 2-tailed (*$P < 0.05$; **$P < 0.01$, $n = 5$–7).

who responded to CIT (Figure 2B). In addition to this patient, we measured and compared the frequency of CX3CR1$^+$Granzyme B$^+$ cells in other responders and nonresponders before and after chemotherapy during CIT. Similar to Figure 2B, the frequency of CX3CR1$^+$Granzyme B$^+$ cells increased in responders compared with nonresponders after chemotherapy (Figure 2C). We also compared the proliferation and cytotoxic T lymphocyte (CTL) function of CX3CR1-expressing or -nonexpressing CD8$^+$ T cells collected from responders before and after chemotherapy during CIT. As shown in Figure 2, D and E, CX3CR1$^+$CD8$^+$ T cells preserved more functional CTLs compared with CX3CR1$^-$CD8$^+$ T cells. The levels of proliferation are comparable in CX3CR1$^+$ and CX3CR1$^-$ CD8$^+$ T cells before chemotherapy, while their proliferation tended to decrease in both populations of CD8$^+$ T cells after chemotherapy. Our results suggest that CX3CR1 identifies PD-1 therapy–responsive CD8$^+$ T cells that can withstand chemotherapy and preserve their CTL functions.

The drug efflux ability of CX3CR1$^+$CD8$^+$ T cells. To define the mechanisms by which CX3CR1$^+$CD8$^+$ T cells withstand chemotherapy, we examined the role of drug transporters in CX3CR1$^+$CD8$^+$ T cells. It has been reported that high multidrug efflux mediated by drug transporters enables CD8$^+$ T cells to survive cytotoxic chemotherapy (29). To determine whether high efflux capacity contributes to the survival of CX3CR1$^+$CD8$^+$ T cells during chemotherapy treatment, we measured the efflux of a fluorescent anthracycline (doxorubicin; Dox) in human primary CD8$^+$ T cells isolated from healthy donors. The efflux of Dox increased over time in CX3CR1$^+$CD8$^+$ T cells (Figure 3, A and B). As a consequence of cytotoxic drugs efflux, fewer CX3CR1$^+$CD8$^+$ T cells (efflux cells) underwent apoptosis than CX3CR1$^-$CD8$^+$ T cells (nonefflux cells) (Figure 3C). Since ABC-superfamily multidrug efflux proteins have been previously shown to contribute to chemoresistance in malignant

cells (30), we examined the expression of ABCB1 by CX3CR1$^+$ cells. We found greater expression of ABCB1 in CX3CR1$^+$CD8$^+$ T cells than in CX3CR1$^-$CD8$^+$ T cells (Figure 3D). In addition, CX3CR1$^+$ABCB1$^+$ DP cells demonstrated more efflux of Rh123 (a dye used for measurement of efflux mediated by ABCB1 transporter) than CX3CR1$^-$ABCB1$^-$ double-negative (DN) cells (Supplemental Figure 1; supplemental material available online with this article; https://doi.org/10.1172/jci.insight.97828DS1), suggesting ABCB1 may be a key transporter used by CX3CR1$^+$CD8$^+$ T cells for drug efflux. To determine the role of ABCB1 in T cell drug efflux, we examined whether the efflux of Dox could be blocked by PGP4008, a specific ABCB1 transporter inhibitor (31, 32). The results of Figure 3E show that PGP4008 at doses of 5–10 μM significantly suppressed the efflux of Dox by CX3CR1$^+$CD8$^+$ T cells. Accordingly, the addition of PGP4008 increased the apoptosis of CX3CR1$^+$CD8$^+$ T cells in culture (Figure 3F), suggesting that ABCB1 contributes to the survival of T cells during chemotherapy.

Since the pharmacodynamics of Dox may not exactly reflect the efflux of CP and these drugs cannot be directly tracked due to their lack of fluorescent capability, we examined the impact of the drug transporter inhibitor on the function of T cells in the presence of CP. We hypothesized that drug transporter inhibition would dampen T cell function due to the reduced ability of T cells in CP efflux. We incubated the ABCB1 transporter inhibitor (PGP4008) with resting or activated human primary CD8$^+$ T cells in vitro in the presence of CP. T cell function was measured by their degranulation (CD107a expression) and intracellular IFN-γ production. PGP4008 significantly inhibited the function of CX3CR1$^+$CD8$^+$ T cells in the presence of CP (Figure 3G) but not in the absence of CP (Figure 3H). Our results imply that CX3CR1$^+$CD8$^+$ T cells may use the ABCB1 transporter to efflux cytotoxic drugs in order to withstand chemotherapy and retain their CTL function.

CX3CR1$^+$Granzyme B CD8$^+$ T cells increased in tumors after effective CIT. To examine whether the frequency of CX3CR1$^+$Granzyme B$^+$CD8$^+$ T cells reflects the therapeutic effects of CIT, we designed 2 schedules of CIT according to the 2 phases of T cell responses to tumors in an animal model (19, 33). In this model, the frequency of tumor-antigen–specific effector CD8$^+$ T cells peaked at days 10–14 (after tumor inoculation) within tumor tissues (19, 33). According to the kinetics of T cell responses within tumors, we defined the expansion phase (days 7–9) and effector phase (days 10–14) of antitumor responses. Anti–PD-1/L1 therapy was given to cover the expansion and effector phases according to the dynamic expression of PD-1 (33). CP Chemotherapy was given at either phase in order to evaluate its impact on T cell responses (Figure 4A). We found that the addition of CP on day 10 (effector phase), but not on day 7 (expansion phase), significantly suppressed the tumor growth of B16F10 mouse melanoma in combination with anti-PD-1/L1 therapy (Figure 4B), and it prolonged the survival of treated mice (Figure 4C). Accordingly, the frequency of CX3CR1$^+$Granzyme B$^+$CD8$^+$ effector T cells had the highest increase in the group treated with CP plus anti–PD-1/L1 on day 10 compared with groups treated with either CP alone or with anti–PD-1/L1 on day 7 (Figure 4D). Of note, the frequency of CX3CR1$^+$Granzyme B$^+$CD8$^+$ T cells was higher in mice treated with CP on day 10 than on day 7, even without combination with anti-PD/L1 (Figure 4D), suggesting that the timing of chemotherapy is critical in the success of CIT. In line with PD-1 blockade prior to chemotherapy, the tumor growth in PD-1–KO mice was also significantly suppressed by CP chemotherapy compared with WT mice (Figure 4E). Taken together, our results suggest that PD-1 blockade prior to chemotherapy may sensitize tumors to CIT.

CX3CR1 is required for CD8$^+$ CTL to reject tumors during CIT. Since CX3CR1 is a chemokine receptor that is critical for T cell accumulation at tumor sites (34), we examined whether CX3CR1 expression is required to mediate antitumor activity. We grew tumor cells in CX3CR1-KO mice, followed by treatment of CIT (day 10 CP plus anti–PD-1/L1). In contrast to WT mice, CIT did not suppress tumor growth in CX3CR1-KO mice (Figure 5, A and B). In addition, the frequency of CD107a$^+$IFN-γ$^+$CD8$^+$ effector T cells within tumors significantly decreased in CX3CR1-KO mice compared with WT mice (Figure 5C). To address whether the CD8$^+$ T cells specially require CX3CR1 to mediate antitumor function, we performed adoptive transfer of activated OT-1 CD8$^+$ T cells for the treatment of a B16-OVA tumor model. We found that the transfer of CX3CR1$^+$, but not CX3CR1$^-$, CD8$^+$ T cells significantly suppressed tumor growth (Figure 5D), suggesting that CX3CR1 expression is critical for CD8$^+$ CTL to mediate tumor rejection. To further examine the role of CX3CR1 in CD8$^+$ T cells, we compared the gene transcriptome between WT and CX3CR1-KO CD8$^+$ T cells at resting or activated stages. As shown in Figure 5E, 3 genes (bmf, ccr5, and mr1) consistently increased in CX3CR1-KO CD8$^+$ T cells, regardless of their activation status. Among them, the bmf gene codes a protein (Bcl-2 modifying factor) that functions as an apoptotic activator (35). In addition, CCR5 has been reported to induce T cell apoptosis (36, 37). Thus, CX3CR1 expression may help CD8$^+$ T cells to survive through suppressing the transcription of apoptotic molecules (bmf and ccr5). Taken together, our results indicate that CX3CR1 is required for CD8$^+$ T cells to reject tumors, as CX3CR1 may help T cell migration and survival at tumor sites.

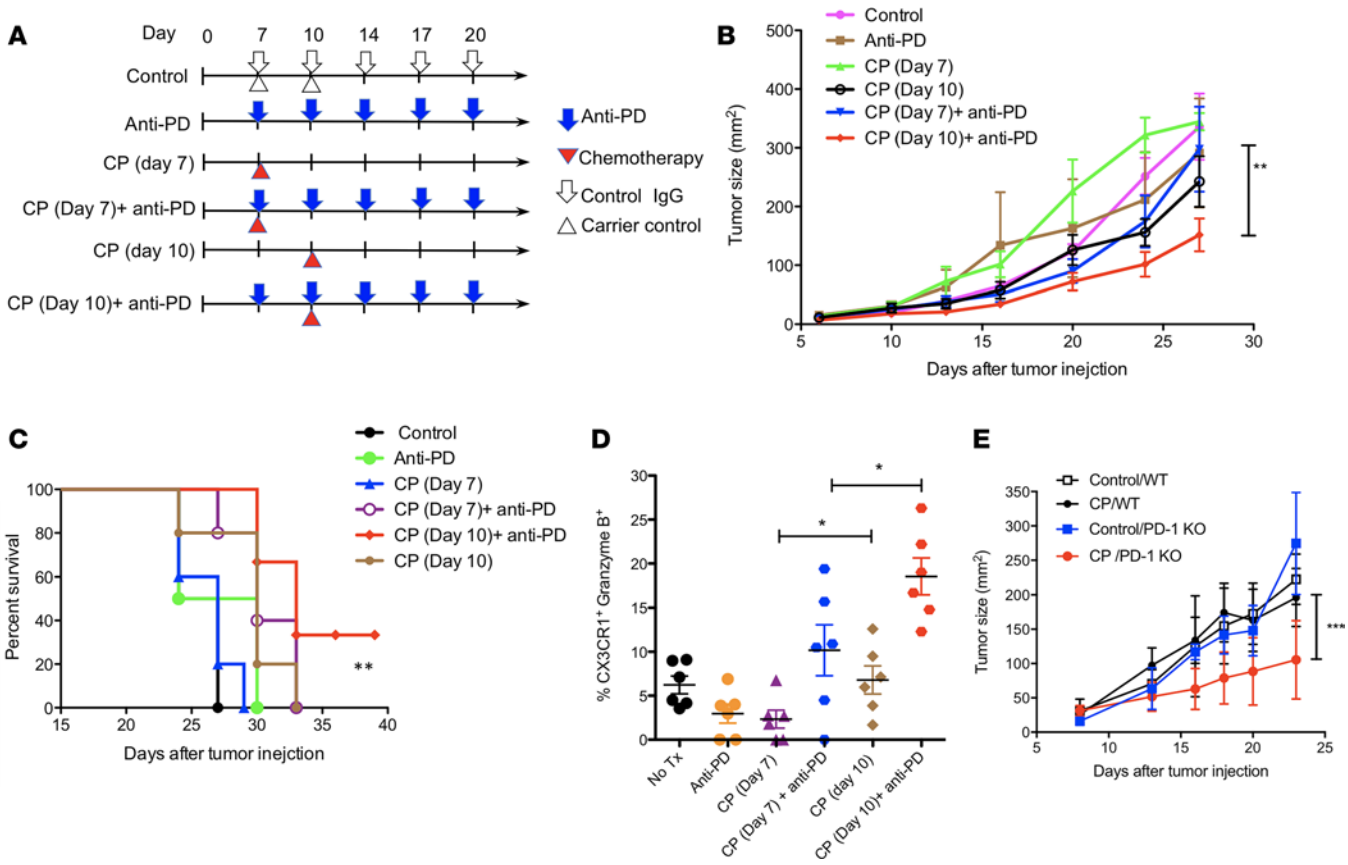

Figure 4. CX3CR1⁺Granzyme B⁺CD8⁺ T cells increased after chemoimmunotherapy. Once B16F10 mouse melanoma tumors were palpable on day 7 after tumor injection, animals were randomly assigned to treatment groups. (**A**) Schedule of treatments. Mice were treated with i.p. injection of anti–PD-1 and –PD-L1 antibody (at 100 μg of each antibody) and collectively indicated as anti-PD IgG for a total of 5 doses at 3-day intervals. Carboplatin (40 μg/g) and paclitaxel (10 μg/g body weight) (collectively indicated as CP) were injected i.p. once either on day 7 or on day 10 after tumor injection. (**B**) Tumor growth. Data show the mean ± SEM of 5 mice per group; $^{**}P < 0.01$ compared between day 7 and 10 treatment with CP plus anti-PD (2-way ANOVA). (**C**) The survival curve of treated animals as in **B**. $^{*}P < 0.05$ compared between control and anti-PD plus day 10 CP (log-rank test). (**D**) Frequency of CX3CR1⁺Granzyme B⁺CD8⁺ T cells was measured in CD11a^{hi}CD8⁺ cells isolated from tumor tissues on day 16 after tumor injection ($^{*}P < 0.05$, $n = 6$, 2-way ANOVA). (**E**) B16F10 tumor growth in WT and PD-1–KO mice after treatment with CP) as in **B** on day 8 after tumor injection. One of 2 independent experiments ($^{***}P < 0.001$, $n = 3$–5, 2-way ANOVA).

Discussion

Our studies show that CX3CR1 identifies a subset of PD-1 therapy–responsive CD8⁺ T cells that withstands chemotherapy and expands after CIT. CX3CR1⁺CD8⁺ T cells demonstrated an effector memory phenotype and may eventually execute tumor rejection due to their abilities of drug efflux (ABCB1 transporter), cytolytic activity (granzyme B and perforin), and migration to and retention (CX3CR1 and CD11a) at tumor sites.

The selection of CX3CR1 as a potential marker to identify a subset of PD-1 therapy–responsive CD8⁺ T cells is of particular importance. CX3CR1 is a receptor of the chemokine CX3CL1 (fractalkine) (38). CX3CR1 correlates with the degree of effector CD8⁺ T cell differentiation, and CX3CR1⁺ cells are the predominant memory T cells surveying peripheral tissues (39). In addition, CX3CR1⁺CD8⁺ T cells define the terminally differentiated cytotoxic effector cells ready to infiltrate inflamed tissues (39, 40). The high expression of CX3CL1 within tumor tissues leads to tumor rejection due to the increased attraction and retention of antitumor innate immune cells and T cells (34, 41–46). Since CD8⁺ T cells need CX3CR1 to migrate and retain at tumor sites (34, 41) (Figure 5), CX3CR1 expression may help us identify potential tumor-attacking T cells in the peripheral blood. We found PD-1 expression was higher in CX3CR1⁺CD8⁺ T cells (Figure 1C), as was transcription of KLRG1 (Figure 1B), suggesting CX3CR1⁺CD8⁺ T cells are PD-1 therapy–responsive effector CD8⁺ T cells capable of entering tumor tissues and executing tumor rejection. In line with our observations, Wallin et al. reported that CX3CR1⁺CD8⁺ T cells increased in the peripheral blood of patients with renal cell carcinoma after treatment with anti–PD-L1 (atezolizumab) and anti-VEGF (bevacizumab) (47), suggesting CX3CR1⁺CD8⁺ T

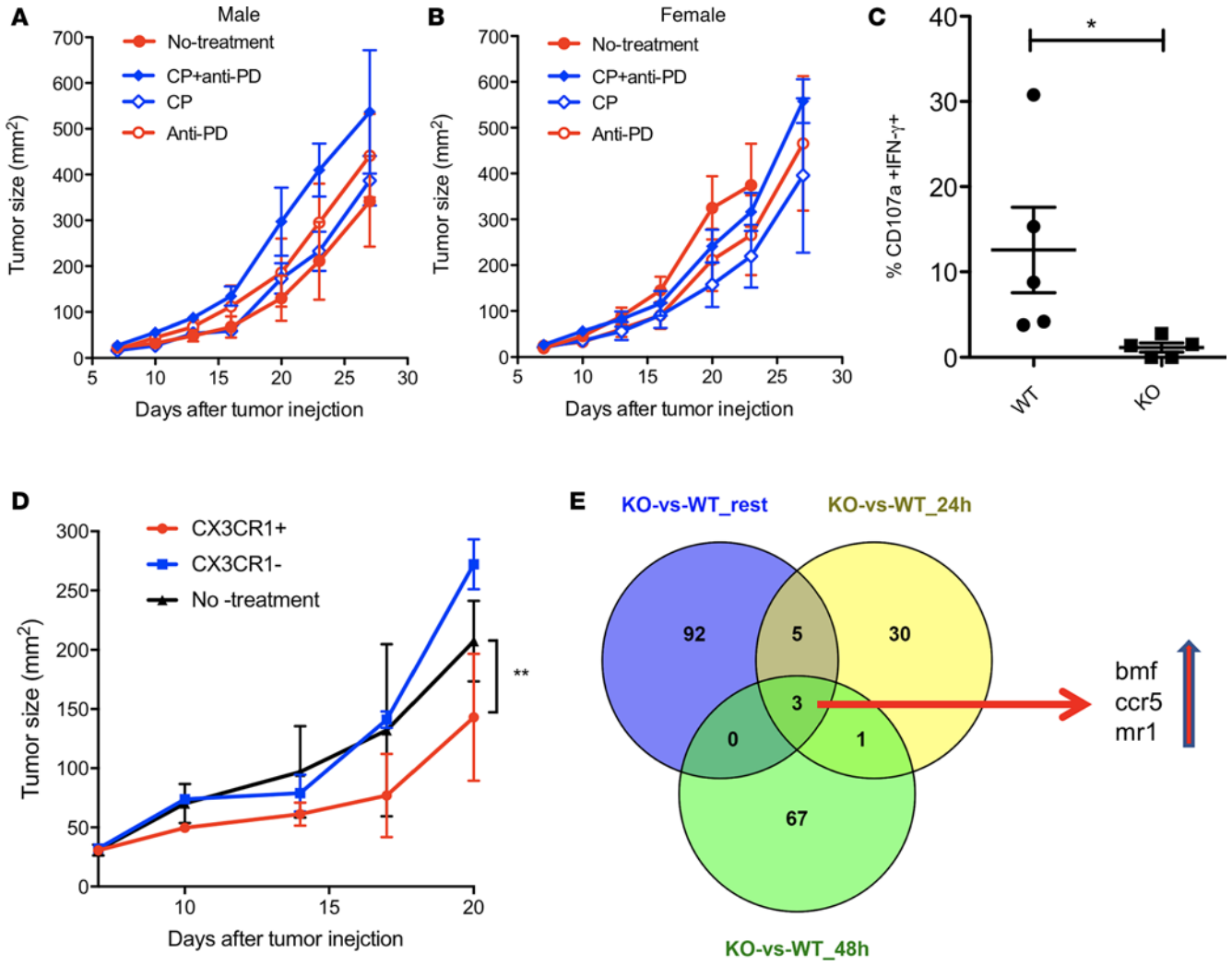

Figure 5. CX3CR1 is required for CD8⁺ CTL to reject tumors during chemoimmunotherapy. CX3CR1-deficient (**A**, male mice; **B**, female mice) mice were injected with B16F10 tumor cells and were treated with i.p. injection of anti–PD-1 and PD-L1 antibody (at 100 μg of each antibody and collectively indicated as anti-PD) or control IgG for a total of 5 doses at 3-day intervals on day 7 after tumor injection. Carboplatin (40 μg/g) and paclitaxel (10 μg/g body weight) (collectively indicated as CP) were injected i.p. once on day 10 after tumor injection. Data show the mean ± SEM of 5 mice per group. (**C**) Frequency of $CD107a^{+}IFN\text{-}\gamma^{+}$ among $CD11a^{hi}CD8^{+}$ T cells isolated from tumor tissues decreased in CX3CR1-KO mice compared with WT mice. $^{*}P < 0.05$ (Mann-Whitney *U* test, 2-tailed, $n = 5$). (**D**) Adoptive transfer of $CX3CR1^{+}$ OT-1 $CD8^{+}$ T cells, but not $CX3CR1^{-}$ OT-1 $CD8^{+}$ T cells, suppressed the growth of B16-OVA tumors. Data show the mean ± SEM of 5 mice per group. $^{**}P < 0.01$ (2-way ANOVA). One of 2 independent experiments was shown. (**E**) Venn diagram shows 3 genes upregulated in CX3CR1-KO $CD8^{+}$ T cells compared with WT $CD8^{+}$ T cells, and the upregulation of these 3 genes was shared among groups of 3 statuses (resting, 24-hour, and 48-hour activation with anti-CD3/CD28 beads in vitro).

cells are responsive to PD-1/L1 blockade therapy. Although peripheral blood provides us a noninvasive way to detect and monitor $CX3CR1^{+}$Granzyme $B^{+}CD8^{+}$ T cells, the presence of $CX3CR1^{+}$Granzyme B^{+} T cells in melanoma tissues (Figure 1E) suggests that tumor biopsies are also valuable to further define the functions of this T cell subset in regards to the clinical response to CIT.

It is interesting that chemotherapy given to patients after anti–PD-1 therapy demonstrated clinical success when neither anti–PD-1 nor chemotherapy alone cause tumor regression (2, 3, 7). However, many have accepted that chemotherapy given before immunotherapy would work better than when given after immunotherapy for several reasons. One reason is that chemotherapy causes immunogenic tumor death that improves T cell priming (16). Another reason is that T cell toxicity is avoided when chemotherapy is given before immunotherapy because proliferating T cells that expand after immunotherapy are more sensitive to cytotoxic drugs. Unexpectedly, studies — including ours — show that chemotherapy after immunotherapy also achieves clinical responses in both lung cancer and melanoma (2, 3, 6, 7). We hereby reported a new mechanism that can explain the promising clinical outcomes

of CIT. We demonstrated that CX3CR1$^+$CD8$^+$ T cells can withstand the toxicity of chemotherapy and preserve their CTL function (Figure 2). One reason is that CX3CR1 identifies effector CD8$^+$ T cells that are not actively proliferating during CIT (Figure 2E) (28), as most chemotherapy reagents are cytotoxic to proliferating cells, including normal cells. Another reason is that CX3CR1$^+$CD8$^+$ T cells are capable of drug efflux (Figure 3). CX3CR1$^+$CD8$^+$ T cells express ABCB1 (Figure 3), a member of the ABC superfamily of drug transporters (30). Inhibition of ABCB1 not only blocked drug efflux of CX3CR1$^+$CD8$^+$ T cells, but also increased the apoptosis of CX3CR1$^+$CD8$^+$ T cells in the presence of chemotherapy reagents (Figure 3). In addition, CX3CR1 may help T cell survival by suppressing the transcription of the apoptotic molecule bmf (Figure 5E). Similar prosurvival function of CX3CR1 has been reported in nonimmune cells through the PI3K/AKT/ERK pathway (48, 49). Future studies will be directed to define whether bmf expression is regulated by the ERK pathway (35) as a downstream signal of CX3CR1 in CD8$^+$ T cells.

In line with our clinical findings, our preclinical studies also show that chemotherapy after initial PD-1/L1 blockade significantly suppressed tumor growth and increased CX3CR1$^+$Granzyme B$^+$CD8$^+$ T cells within tumor tissues (Figure 4). The requirement of CX3CR1 in antitumor activity was confirmed by 2 in vivo experiments that we performed. First, we found that CX3CR1-KO mice did not respond to CIT and had a reduced frequency of functional CD8$^+$ CTLs within tumors (Figure 5). Our results are in agreement with a previous study reporting a defective antitumor response in CX3CR1-KO mice that have defects in production of IFN-γ by immune cells (42). Second, we found the transfer of CX3CR1$^+$CD8$^+$ T cells, but not CX3CR1$^-$CD8$^+$ T cells, suppressed tumor growth (Figure 5). Our results added more evidence in support of a critical role of the Fractalkine/CX3CR1 pathway in T cell–mediated antitumor function (50, 51). Taken together, our clinical and preclinical studies suggest that the preexisting or increase of CX3CR1$^+$CD8$^+$ T cells plays a key role in tumor rejection in response to CIT.

Our study is limited by the small numbers of patient samples that did not allow us to determine whether the frequency of CX3CR1$^+$Granzyme B$^+$CD8$^+$ T cells can predict clinical responses to CIT after initial anti–PD-1 therapy failure. However, this important question will be addressed and evaluated in our future studies, which will recruit more patients who receive CIT as a treatment for advanced melanoma and lung cancer. Of note, although our studies focused on paclitaxel and carboplatin, since not all chemotherapy drugs work through the same mechanisms, stratification by treatment is warranted to evaluate the benefit of immunotherapy combined with specific chemotherapy drugs in the context of their unique impact on antitumor immune responses.

In summary, our study provides insights into the cellular mechanisms responsible for the success of CIT in cancer patients who do not respond to initial anti–PD-1 therapy. Our study suggests that strategies to monitor and increase the frequency of CX3CR1$^+$CD8$^+$ T cells may help to design effective CIT to overcome cancer resistance to immune checkpoint blockade therapy.

Methods

Patient information. Peripheral blood and tissue samples for this study were collected after written consents were obtained. Clinical course, treatment information, and outcomes in patients with metastatic melanoma who did not respond to anti–PD-1 single agent therapy were retrospectively collected. Patients who failed initial PD-1 therapy were subsequently treated with salvage CP paclitaxel and carboplatin combination in addition to PD-1 blockade, regardless of BRAF mutant status. Response to treatment was evaluated according to standard clinical practice guidelines using RECIST criteria.

Flow analysis of human T cells isolated from peripheral blood. Peripheral blood mononuclear cell (PBMC) samples were collected from healthy donors or patients with melanoma at Mayo Clinic. Antibodies for CD45 (clone HI30, catalog 304006), CD3 (clone OKT3, catalog 317344), CX3CR1 (clone 2A9-1, catalog 341616), CD11a (clone HI111, catalog 301212), and PD-1 (clone EH12.2H7, catalog 329904) were purchased from BioLegend; CD8 (clone RPA-T8, catalog 557746) antibody was purchased from BD Biosciences; anti–human granzyme B (clone GB11, catalog NBP1-50071PCP) was purchased from Novus; and Ki67(clone B56, catalog 562899) antibody was purchased from BD Biosciences. CD8$^+$ T cells were first stained for surface markers (including CX3CR1) followed by intracellular staining for granzyme B. To initiate CTL function, cells were briefly stimulated with PMA and ionomycin (MilliporeSigma) for 5 hours in the presence of anti-CD107a antibody (clone H4A3, catalog 328642, BioLegend) followed by intracellular staining of anti–IFN-γ antibody (clone 4S.B3, catalog 502509, BioLegend). Flow cytometry analysis was performed using FlowJo software (Tree Star Inc.).

RNA-seq and bioinformatics assay. Total RNA was extracted with RNeasy Mini kit (Qiagen) and checked for quality by Bioanalizer (RNA 6000 Pico kit; Agilent Technologies, Inc.). A total of 1 ng RNA was used to generate double-stranded cDNA using the SMARTer Ultra Low RNA kit from Illumina. For RNA-seq library construction, 250 pg of cDNAs were used to construct indexed libraries using Nextera XT DNA Sample Preparation kit (Illumina). Full-length double-stranded cDNA and the libraries were quantified by Bioanalyzer (High Sensitivity DNA analysis kit, Agilent) and Qubit (dsDNA BR Assay kits, Invitrogen). The libraries were sequenced using the 101 base paired-end protocol on Illumina HiSeq 2000. FASTQ formatted raw files from each sample were mapped and aligned to reference hg19.

The MAP-RSeq workflow for mRNA began with raw FASTQ reads and aligned them using TopHat2 to the relevant genome. The BAM files thus obtained were passed through other tools for further analysis. Fusion detection was done using a module from the TopHat aligner, called TopHat-Fusion. Raw and normalized gene and exon counts were generated by FeatureCounts, which used the ENSEMBL GRCh38.78 gene definitions. Finally, the RSeQC module created a variety of QC plots and graphs, which ensured that the quality of samples was good and reliable to be used in further downstream analyses like differential expression and pathway analysis. The R-based tool from Bioconductor, edgeR v3.8.6, was used to perform the differential expression analysis comparing the various sample groups. We considered genes in mRNA that had an absolute $\log_2$ fold change >1.5 to be significantly differentially expressed. Heatmaps were created using the heatmap.2 function of the gplots package from R. The original RNA-seq data were deposited at NCBI Gene Expression Omnibus (GEO) website with the accession number GSE111981 (http://www.ncbi.nlm.nih.gov/geo/query/acc.cgi?acc=GSE111981).

Immunochemistry staining of melanoma tissues. Paraffin-embedded tissue sections were cut into 5-μm sections and deparaffinized in xylene and rehydrated in a graded series of alcohols. Antigen retrieval was performed by heating tissue sections in Target Retrieval Solution pH 6.0 (Dako, S1699) at 98°C for 30 minutes. Sections were cooled on the bench for 20 minutes, washed in running DH_20 for 5 minutes, and incubated for 5 minutes in wash buffer. Sections were blocked for 5 minutes with Endogenous Peroxidase Block (Dako, S2001), washed, and blocked for 5 minutes in Protein Block Serum Free (Biocare Medical, X0909). Slides were incubated for 1 hour in mouse monoclonal anti–human granzyme B (Dako, M7235) diluted 1:50 in Antibody Diluent with Background Reducers (Dako, 3022). Sections were washed and incubated 15 minutes each in mouse probe and mouse polymer alkaline phosphatase (AP) (Mach 3 Mouse AP Polymer Detection Kit, Biocare Medical, M3M532L). Sections were incubated for 5 minutes in Warp Red Chromogen (Biocare Medical, WR806H) for visualization. Subsequently, sections were incubated for 5 minutes in 80°C Citrate Buffer (pH 6), rinsed in wash buffer, and incubated in Protein Block Serum Free for 5 minutes. Rabbit anti–human CX3CR1 (Invitrogen, PA5-32713) was applied to sections at 1:500 dilution and incubated for 1 hour at room temperature. Sections were washed and incubated for 15 minutes each in rabbit probe and rabbit polymer HRP (Mach 3 Rabbit HRP Polymer Detection kit, Biocare Medical, M3R531L) and were visualized for 1 minute in DAB (Biocare Medical, BDB2004L). Sections were counterstained and coverglass mounted with Permount (Thermo Fisher Scientific). All chemicals used from Fisher Scientific.

Stimulation and culture of human T cells. Human $CD8^+$ T cells were purified with human $CD8^+$ T cell enrichment Kit (Stemcell Technologies). $CD8^+$ T cells were incubated with chemotherapy drugs alone or with T cell activators (Dynabeads, human T-activator CD3/CD28 beads) for 24–48 hours, followed with staining for CX3CR1 and granzyme B. The drugs are as follows: paclitaxel, carboplatin, or Dox. All these reagents are purchased from the Mayo Clinic pharmacy. ABCB1 inhibitor PGP4008 was purchased from Enzo Life Sciences.

Drug efflux assay in T cells. Human primary $CD8^+$ T cells were isolated from peripheral blood and incubated (loading) with Rh123 (10 μg/ml) on ice for 30 minutes or Dox (1 μg/ml) at 37°C for 60 minutes in water bath. After the loading process, cells were washed and cultured at 37°C for 60 minutes (efflux), followed with staining for cell-surface markers and analysis by flow cytometry. The ABCB1 inhibitor PGP-4008 was added at 1–5 μM during the process of efflux.

Animal models for CIT. Both WT and CX3CR1-KO mice in C57BL/6 background were purchased from the Jackson Laboratory, PD-1–KO mice were provided by T. Honjo (Kyoto University, Kyoto, Japan) and maintained under pathogen-free conditions in the animal facility at Mayo Clinic Comparative Medicine Department. B16F10 (1×10^5 cells) mouse melanoma cells were s.c. injected into mice in the right flank, followed with treatment of i.p. injection of anti–PD-1 (clone G4) and PD-L1 antibody (clone 10B5) (52) or control IgG at 100 μg of each starting on day 7 for a total of 5 doses at 3-day intervals. Both G4 and 10B5 antibodies were produced at Mayo Clinic Antibody Core facility. Carboplatin (40 μg/g) plus paclitaxel (10

μg/g body weight) were injected i.p. once either on day 7 or on day 10 after tumor injection. CTL function of tumor-infiltrating $CD8^+$ T cells was measured by briefly stimulating them with PMA and ionomycin (MilliporeSigma) for 5 hours in the presence of anti-CD107a antibody (clone 1D4B, catalog 121606, BioLegend) followed with intracellular staining of anti–IFN-γ antibody (clone XMG1.2, catalog 505808, BioLegend). Perpendicular tumor diameters were measured using a digital caliper (Carbon Fiber Composite, Fisher Scientific), and tumor sizes were calculated as length × width. Tumor growth was evaluated every 2–3 days until ethical endpoints, when all mice were euthanized in compliance with animal care guidelines.

T cell transfer therapy. Spleen cells isolated from OT-1 mice that express OVA-antigen–specific TCR were cultured with OVA peptide (1 μg/ml) and rhIL-2 (10 IU/ml) for 48 hours. Both $CX3CR1^+$ and $CX3CR1^-$ $CD8^+$ T cells were sorted after culture on the day of T cell transfer. Once B16-OVA mouse melanoma established around day 7 after tumor cell injection (5×10^5 cells per mouse, s.c.), they were treated with intratumor injection of either $CX3CR1^+$ or $CX3CR1^-$ $CD8^+$ T cells at equal numbers (2×10^5 to 3×10^5 T cells per mouse) for a total of 3 doses on days of 7, 10, and 13 after tumor injection.

Statistics. Mann-Whitney *U* test was used to compare independent groups (function or subsets of $CD8^+$ T cells). Two-tailed paired *t* test was used to compare PD-1 expression between $CX3CR1^{+/-}$ T cells. The impacts of both chemotherapy or anti–PD-1/L1 antibody on tumor growth were analyzed by 2-way ANOVA. Comparisons of the impact of ABCB1 inhibitors and timing on the efflux of drug were analyzed with 1-way ANOVA due to the numerical independent variables. The survival of animals was analyzed by log-rank Mantel-Cox test. All statistical analyses were performed using GraphPad Prism software 7.0 (GraphPad Software Inc.). $P < 0.05$ was considered statistically significant.

Study approval. The Mayo Clinic ACUC approved all animal experiments. Human blood leukocytes were acquired from anonymous donors from the Blood Transfusion Center at Mayo Clinic who had consented for blood donation. All patients provided signed informed written consent; the study was approved by the Mayo Clinic Rochester IRB and was conducted according to Declaration of Helsinki principles.

Author contributions

HD, YY, RSD, and SNM conceived the study, designed the experiments and analyzed data. YY, RSD, ASM, AAA, SNM, and SSP directed and supervised the clinical studies. SC, XL, WEB, HD, JSJ, and SMH performed the experiments. PC, YL, and JJ performed bioinformatics analyses. YY, RSD, and HD wrote and edited the manuscript with contributions from other authors.

Acknowledgments

We acknowledge the Melanoma Group in the Division of Medical Oncology at Mayo Clinic for providing excellent patient care. This study was supported by NCI R21 CA197878 (HD and RD), NCI R01 CA200551 (SP and HD), NIAID R01 AI095239 (HD), NCI K12 CA090628 (AM), Richard M. Schulze Family Foundation (RD and HD), and the Mayo Clinic Center for Individualized Medicine Biomarker Discovery (IMPRESS) program (HD, RD, AM, and SM).

Address correspondence to: Haidong Dong, Departments of Urology and Immunology, College of Medicine, Mayo Clinic, 200 First Street SW, Rochester, Minnesota 55905, USA. Phone: 507.284.5482; Email: dong.haidong@mayo.edu.

RD's present address is: Division of Hematology and Medical Oncology, Mayo Clinic, Jacksonville, Florida, USA.

1. Coit DG, et al. Melanoma, Version 2.2016, NCCN Clinical Practice Guidelines in Oncology. *J Natl Compr Canc Netw*. 2016;14(4):450–473.
2. Rizvi NA, et al. Nivolumab in Combination With Platinum-Based Doublet Chemotherapy for First-Line Treatment of Advanced Non-Small-Cell Lung Cancer. *J Clin Oncol*. 2016;34(25):2969–2979.
3. Langer CJ, et al. Carboplatin and pemetrexed with or without pembrolizumab for advanced, non-squamous non-small-cell lung cancer: a randomised, phase 2 cohort of the open-label KEYNOTE-021 study. *Lancet Oncol*. 2016;17(11):1497–1508.
4. Yan Y, et al. The Mayo Clinic experience in patients with metastatic melanoma who have failed previous pembrolizumab treatment. *J Clin Oncol*. 2016;34(15_suppl);e21014.
5. Flaherty KT, et al. Phase III trial of carboplatin and paclitaxel with or without sorafenib in metastatic melanoma. *J Clin Oncol*. 2013;31(3):373–379.

6. Park SE, Lee SH, Ahn JS, Ahn MJ, Park K, Sun JM. Increased Response Rates to Salvage Chemotherapy Administered after PD-1/PD-L1 Inhibitors in Patients with Non-Small Cell Lung Cancer. *J Thorac Oncol*. 2018;13(1):106–111.
7. Ogawara D, et al. Remarkable response of nivolumab-refractory lung cancer to salvage chemotherapy. *Thorac Cancer*. 2018;9(1):175–180.
8. Zitvogel L, Apetoh L, Ghiringhelli F, Kroemer G. Immunological aspects of cancer chemotherapy. *Nat Rev Immunol*. 2008;8(1):59–73.
9. Sampson JH, et al. Greater chemotherapy-induced lymphopenia enhances tumor-specific immune responses that eliminate EGFRvIII-expressing tumor cells in patients with glioblastoma. *Neuro-oncology*. 2011;13(3):324–333.
10. Williams KM, Hakim FT, Gress RE. T cell immune reconstitution following lymphodepletion. *Semin Immunol*. 2007;19(5):318–330.
11. Dummer W, et al. T cell homeostatic proliferation elicits effective antitumor autoimmunity. *J Clin Invest*. 2002;110(2):185–192.
12. Ghiringhelli F, et al. Metronomic cyclophosphamide regimen selectively depletes CD4+CD25+ regulatory T cells and restores T and NK effector functions in end stage cancer patients. *Cancer Immunol Immunother*. 2007;56(5):641–648.
13. Neyns B, Tosoni A, Hwu WJ, Reardon DA. Dose-dense temozolomide regimens: antitumor activity, toxicity, and immunomodulatory effects. *Cancer*. 2010;116(12):2868–2877.
14. Mackall CL, Fry TJ, Gress RE. Harnessing the biology of IL-7 for therapeutic application. *Nat Rev Immunol*. 2011;11(5):330–342.
15. Alizadeh D, Larmonier N. Chemotherapeutic targeting of cancer-induced immunosuppressive cells. *Cancer Res*. 2014;74(10):2663–2668.
16. Bezu L, et al. Combinatorial strategies for the induction of immunogenic cell death. *Front Immunol*. 2015;6:187.
17. Tumeh PC, et al. PD-1 blockade induces responses by inhibiting adaptive immune resistance. *Nature*. 2014;515(7528):568–571.
18. Gros A, et al. PD-1 identifies the patient-specific $CD8^+$ tumor-reactive repertoire infiltrating human tumors. *J Clin Invest*. 2014;124(5):2246–2259.
19. Liu X, et al. Endogenous tumor-reactive CD8+T cells are differentiated effector cells expressing high levels of CD11a and PD-1 but are unable to control tumor growth. *Oncoimmunology*. 2013;2(6):e23972.
20. Dronca RS, et al. T cell Bim levels reflect responses to anti-PD-1 cancer therapy. *JCI Insight*. 2016;1(6):e86014.
21. Robert C, et al. Pembrolizumab versus Ipilimumab in Advanced Melanoma. *N Engl J Med*. 2015;372(26):2521–2532.
22. Robert C, et al. Nivolumab in previously untreated melanoma without BRAF mutation. *N Engl J Med*. 2015;372(4):320–330.
23. Ribas A, et al. Association of Pembrolizumab With Tumor Response and Survival Among Patients With Advanced Melanoma. *JAMA*. 2016;315(15):1600–1609.
24. Liu Y, Janeway CA. Interferon gamma plays a critical role in induced cell death of effector T cell: a possible third mechanism of self-tolerance. *J Exp Med*. 1990;172(6):1735–1739.
25. Prabhu N, et al. Gamma interferon regulates contraction of the influenza virus-specific CD8 T cell response and limits the size of the memory population. *J Virol*. 2013;87(23):12510–12522.
26. Refaeli Y, Van Parijs L, Alexander SI, Abbas AK. Interferon gamma is required for activation-induced death of T lymphocytes. *J Exp Med*. 2002;196(7):999–1005.
27. Huang AC, et al. T-cell invigoration to tumour burden ratio associated with anti-PD-1 response. *Nature*. 2017;545(7652):60–65.
28. Böttcher JP, et al. Functional classification of memory CD8(+) T cells by CX3CR1 expression. *Nat Commun*. 2015;6:8306.
29. Turtle CJ, Swanson HM, Fujii N, Estey EH, Riddell SR. A distinct subset of self-renewing human memory CD8+ T cells survives cytotoxic chemotherapy. *Immunity*. 2009;31(5):834–844.
30. Gottesman MM, Fojo T, Bates SE. Multidrug resistance in cancer: role of ATP-dependent transporters. *Nat Rev Cancer*. 2002;2(1):48–58.
31. Schinkel AH, Jonker JW. Mammalian drug efflux transporters of the ATP binding cassette (ABC) family: an overview. *Adv Drug Deliv Rev*. 2003;55(1):3–29.
32. Walter RB, Raden BW, Cronk MR, Bernstein ID, Appelbaum FR, Banker DE. The peripheral benzodiazepine receptor ligand PK11195 overcomes different resistance mechanisms to sensitize AML cells to gemtuzumab ozogamicin. *Blood*. 2004;103(11):4276–4284.
33. Pulko V, et al. B7-h1 expressed by activated CD8 T cells is essential for their survival. *J Immunol*. 2011;187(11):5606–5614.
34. Kee JY, et al. Antitumor immune activity by chemokine CX3CL1 in an orthotopic implantation of lung cancer modelin vivo. *Mol Clin Oncol*. 2013;1(1):35–40.
35. Shao Y, Aplin AE. ERK2 phosphorylation of serine 77 regulates Bmf pro-apoptotic activity. *Cell Death Dis*. 2012;3:e253.
36. Mellado M, de Ana AM, Moreno MC, Martínez C, Rodríguez-Frade JM. A potential immune escape mechanism by melanoma cells through the activation of chemokine-induced T cell death. *Curr Biol*. 2001;11(9):691–696.
37. Murooka TT, Wong MM, Rahbar R, Majchrzak-Kita B, Proudfoot AE, Fish EN. CCL5-CCR5-mediated apoptosis in T cells: Requirement for glycosaminoglycan binding and CCL5 aggregation. *J Biol Chem*. 2006;281(35):25184–25194.
38. Imai T, et al. Identification and molecular characterization of fractalkine receptor CX3CR1, which mediates both leukocyte migration and adhesion. *Cell*. 1997;91(4):521–530.
39. Gerlach C, et al. The Chemokine Receptor CX3CR1 Defines Three Antigen-Experienced CD8 T Cell Subsets with Distinct Roles in Immune Surveillance and Homeostasis. *Immunity*. 2016;45(6):1270–1284.
40. Nishimura M, et al. Dual functions of fractalkine/CX3C ligand 1 in trafficking of perforin+/granzyme B+ cytotoxic effector lymphocytes that are defined by CX3CR1 expression. *J Immunol*. 2002;168(12):6173–6180.
41. Siddiqui I, Erreni M, van Brakel M, Debets R, Allavena P. Enhanced recruitment of genetically modified CX3CR1-positive human T cells into Fractalkine/CX3CL1 expressing tumors: importance of the chemokine gradient. *J Immunother Cancer*. 2016;4:21.
42. Yu YR, Fong AM, Combadiere C, Gao JL, Murphy PM, Patel DD. Defective antitumor responses in CX3CR1-deficient mice. *Int J Cancer*. 2007;121(2):316–322.
43. Guo J, et al. Fractalkine transgene induces T-cell-dependent antitumor immunity through chemoattraction and activation of dendritic cells. *Int J Cancer*. 2003;103(2):212–220.
44. Park MH, Lee JS, Yoon JH. High expression of CX3CL1 by tumor cells correlates with a good prognosis and increased tumor-infiltrating CD8+ T cells, natural killer cells, and dendritic cells in breast carcinoma. *J Surg Oncol*. 2012;106(4):386–392.
45. Hyakudomi M, et al. Increased expression of fractalkine is correlated with a better prognosis and an increased number of both

CD8+ T cells and natural killer cells in gastric adenocarcinoma. *Ann Surg Oncol*. 2008;15(6):1775–1782.
46. Lavergne E, et al. Fractalkine mediates natural killer-dependent antitumor responses in vivo. *Cancer Res*. 2003;63(21):7468–7474.
47. Wallin JJ, et al. Atezolizumab in combination with bevacizumab enhances antigen-specific T-cell migration in metastatic renal cell carcinoma. *Nat Commun*. 2016;7:12624.
48. White GE, Tan TC, John AE, Whatling C, McPheat WL, Greaves DR. Fractalkine has anti-apoptotic and proliferative effects on human vascular smooth muscle cells via epidermal growth factor receptor signalling. *Cardiovasc Res*. 2010;85(4):825–835.
49. Davis CN, Harrison JK. Proline 326 in the C terminus of murine CX3CR1 prevents G-protein and phosphatidylinositol 3-kinase-dependent stimulation of Akt and extracellular signal-regulated kinase in Chinese hamster ovary cells. *J Pharmacol Exp Ther*. 2006;316(1):356–363.
50. Zeng Y, et al. Fractalkine (CX3CL1)- and interleukin-2-enriched neuroblastoma microenvironment induces eradication of metastases mediated by T cells and natural killer cells. *Cancer Res*. 2007;67(5):2331–2338.
51. Xin H, et al. Antitumor immune response by CX3CL1 fractalkine gene transfer depends on both NK and T cells. *Eur J Immunol*. 2005;35(5):1371–1380.
52. Liu X, et al. B7-H1 antibodies lose antitumor activity due to activation of p38 MAPK that leads to apoptosis of tumor-reactive CD8+T cells. *Sci Rep*. 2016;6:36722.